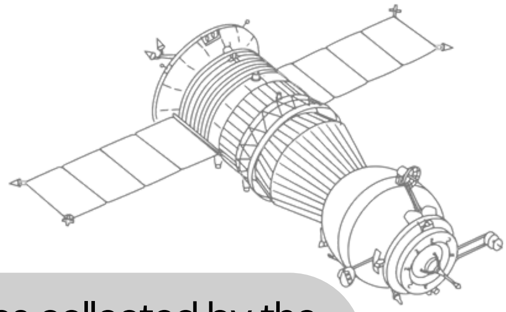

Introduction

Our algorithm achieves a 30cm resolution of images collected by the TMC-2 payload of Chandrayaan 2 using a combination of Deep Learning models and feature enhancement methods. Further, we generate an atlas of the moon as covered by TMC-2, using enhanced images.

1.Super Resolution of Images

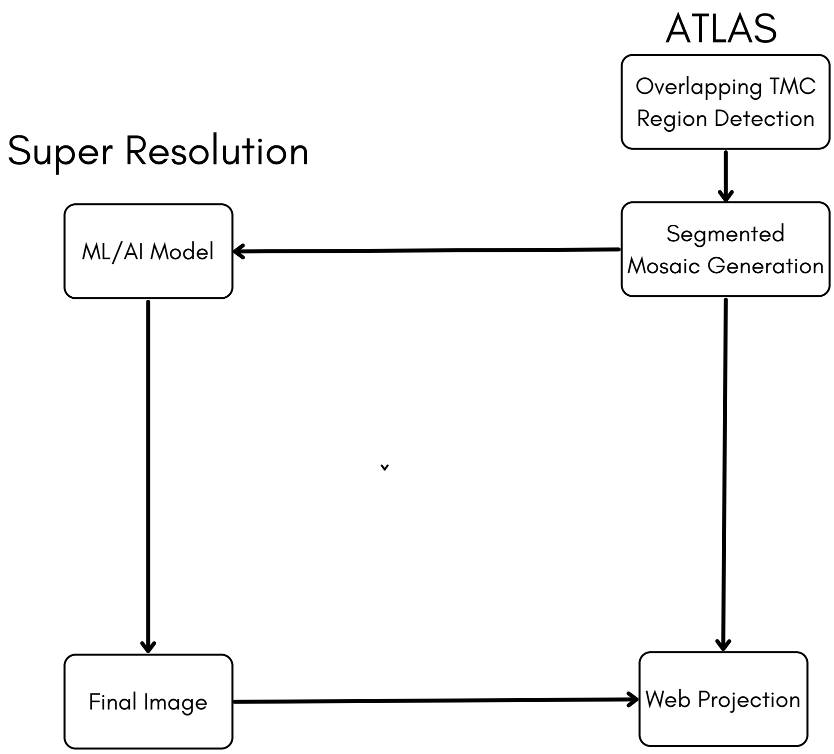

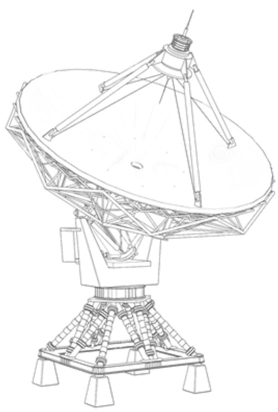

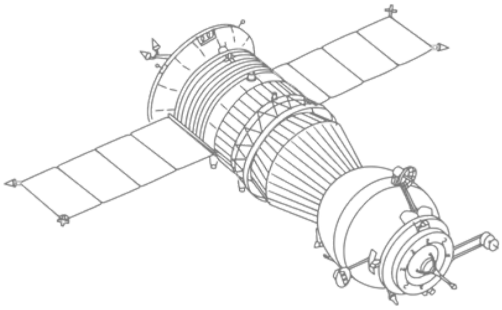

Data collection

We extracted data for three different payloads:
1. TMC 2 of Chandrayan 2: DEM and orthoimages with .png and .tif file extensions
2.OHRC of Chandrayan 2: Calibrated images with .img file extension
3.NAC of LROC: orthoimages with .tif file extension

Model Architecture

Our overall Super-resolution model is a combination of two different algorithms:
1. Interpolation and
2. Deep Learning.

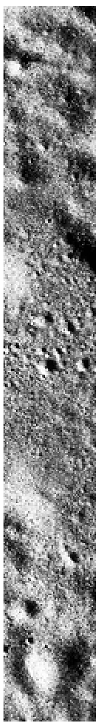

OHRC .png data

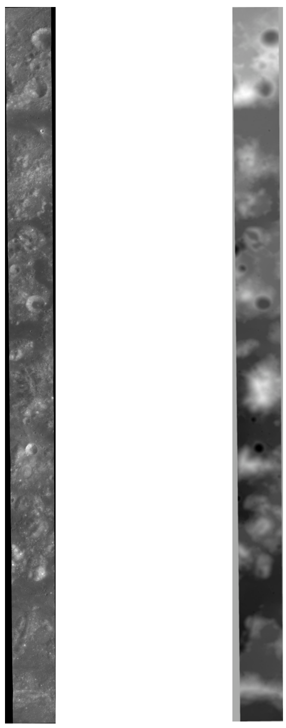

TMC image with corresponding DTM

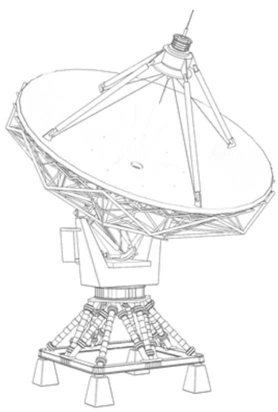

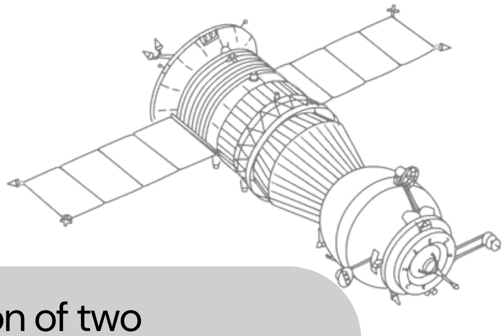

Model Architecture

Our overall Super-resolution model is a combination of two different algorithms:
1. Interpolation and
2. Deep Learning.

Interpolation algorithms

For interpolation, we followed an ensemble approach between 3 interpolation techniques: namely, bicubic interpolation, inter_area interpolation, and inter_nearest interpolation. More specifically, our final image is obtained by a weighted sum of the different interpolation techniques as below:

$$\text{HRImage} = \alpha * F1(LR) + \beta * F2(LR) + \gamma * F3(LR)$$

Where F1, F2, F3 are the 3 interpolation techniques and α, β and γ are the corresponding weighting terms optimized using Optuna under the condition that $\alpha + \beta + \gamma = 1$

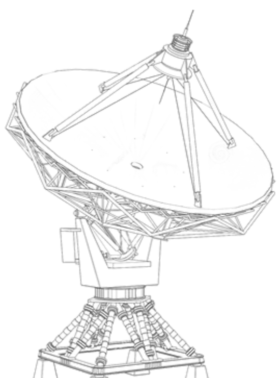

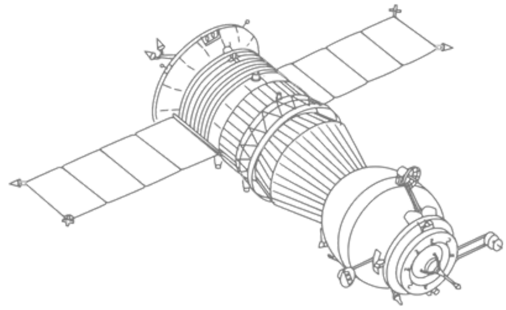

Deep Learning algorithms

Generative Adversarial Networks (GANs) with Turing Test Adversories for Elevation-Centric Image Super-Resolution

Input Data For training

- Original HR Image
- Low Resolution image (Downsized from Original)
- Masks of the craters
- Masks of the hills

Model Architecture

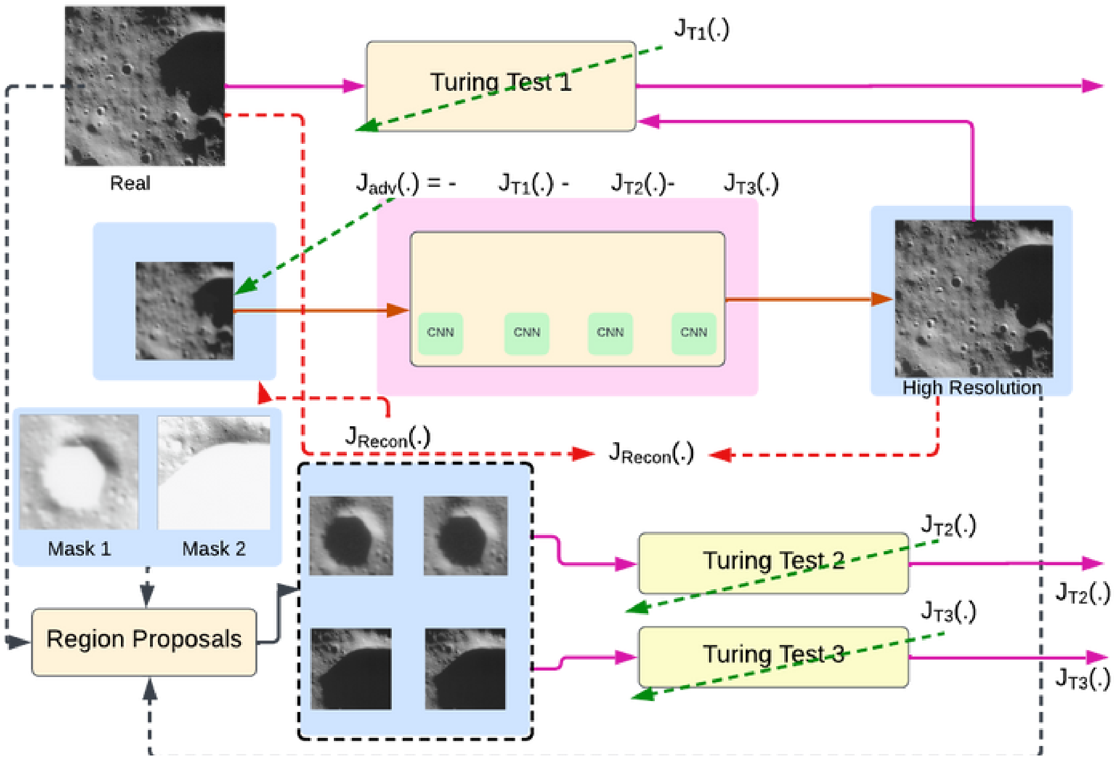

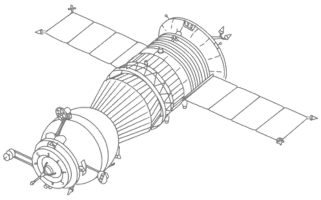

Model Explanation

We modify the conventional discriminator of GANs with a novel turing loss that ensures the model places a special emphasis on the region of interest: in our case the craters and the hills. More specifically, as shown in the figure above, we have a Turing Test 1 (T1) which is trained to discriminate the fake image (SR) from the original image (HR).
The Turing Test 2 (T2) is trained to perform the same discrimination only on the craters. Likewise Turing Test 3 (T3) is trained to discriminate the hills in the lunar surface. We detect the hills and craters from the TMC 2 ortho images using manual annotation of DEM maps of TMC2 data .
The network is trained in 5 stages on the TMC2 images by downsizing them. We perform tiling of the images to pass it to the model.

Improved Hybrid Attention Transformer for Lunar Image Super-Resolution

Input Data For training

- Original High Resolution Image
- Low Resolution image (Downsized from Original Images)

Model Architecture

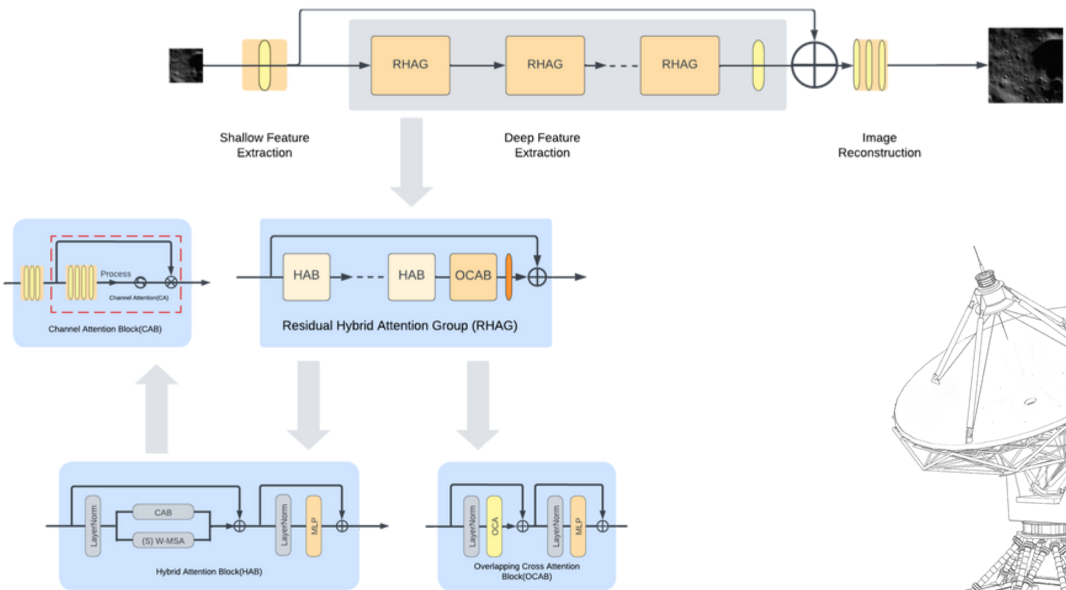

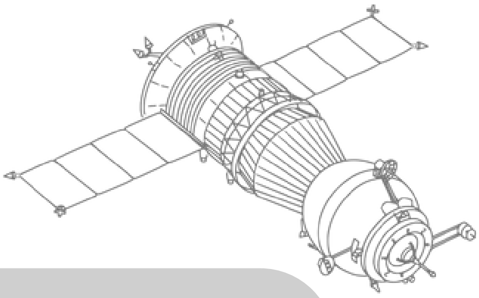

Model Explanation

We suggest a unique Hybrid Attention Transformer to activate more input pixels for reconstruction (HAT). It combines self-attention and channel attention strategies, utilizing their complementing benefits. Additionally, the paper improves the interaction between surrounding window characteristics, we add an overlapping cross-attention module to better aggregate the cross-window information.

Real-ESRGAN: Training Real-World Blind Super-Resolution with Pure Synthetic Data

Input Data For training

- Original High Resolution Image
- Low Resolution image (Downsized from Original Images)

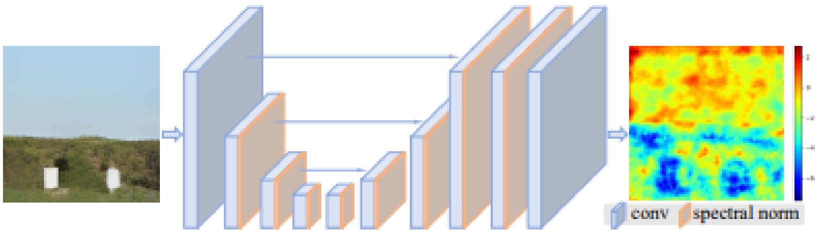

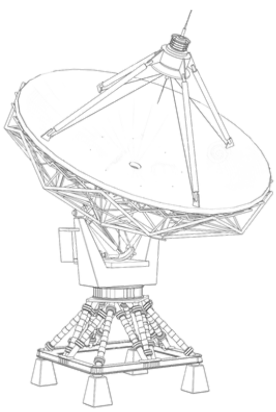

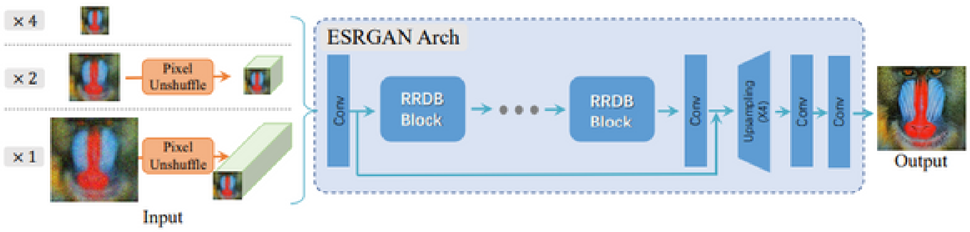

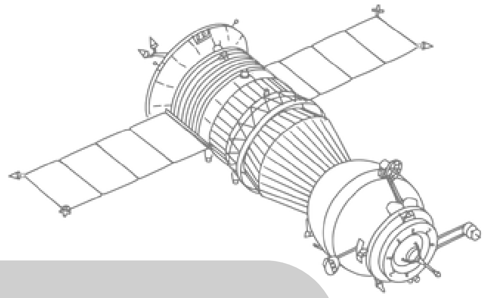

Model Explanation

We adopt a state-of-the art GAN model which uses residual-in-residual dense block in generator and a residual network in the discriminator. To enhance its performance we add a combination of fast fourier transform loss and Frequency Domain Perceptual Loss instead of normal mean square error.

Sharpening and Denoising

Sharpening
The sharpening algorithm also enhanced the noise per pixel of the image, hence we had to use a denoising algorithm to check the signal-to-noise preservation.

Denoising
We use a pre-trained Deep Learning model called NAFNet for Image Denoising

Image comparison

We downsized the original OHRC images 16 times using bicubic interpolation and then we used the proposed algorithms to get super-resolved images. Further, we compared the original image with the super-resolved image to get the following results:

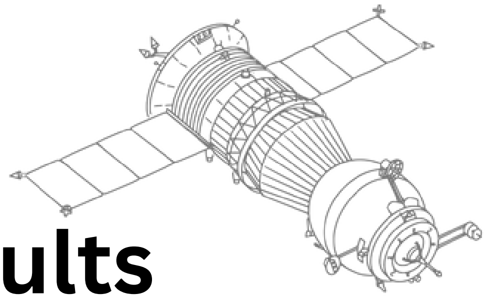

Experimental Results

Model	Inference Time	Architecture	SSIM	FSIM	PSNR	SAM
Bicublc Interpolation	21.8 3	Maths	0.762	0.651	59.014	64.672
SRGAN	55.9 3	GAN	0.812	0.681	59.421	64.659
EDSR	51.8 3	GAN	0.814	0.685	59.482	64.654
WDSR	39.5 3	GAN	0.816	0.687	59.496	64.652
MSRNet	356 to	CNN	0.828	0.691	59.561	64.42
SwinIR	359 3	Transformer	0.858	0.696	59.653	64.39
Attention 2 Attention	35.7 S	Attention	0.812	0.679	59.305	64.663
Real ESRGAN	48.7 S	GAN	0.838	0.689	59.559	64.645
HAT	337s	Transformer	0.88	0.705	59.719	64.635
Lunar T-GAN (Ours) - trained only on 50 images	11s	GAN	0.794	0.672	59.104	64.669

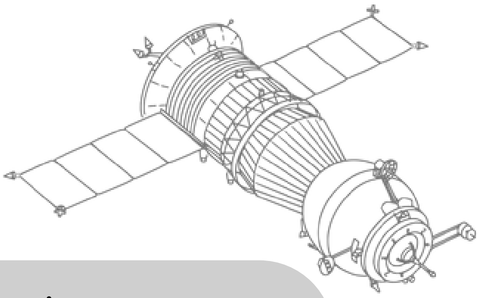

Evaluation of super resolution

Observing the improved data in lunar super-resolution images can provide valuable information about the geological and physical processes that have shaped the moon's surface over time. This can provide a better understanding of the moon's history and evolution, as well as help in planning for future missions to the moon. The high resolution images can also reveal new features and details that were previously not visible, leading to new discoveries and scientific insights.
We have built a variety of algorithms for comparison of physical features obtainable from the lunar images, before and after super-resolution. This conveys the improvement in the detection and analysis of features in the super-resolved images.

There are two major criteria on which the super resolved images have been evaluated:
1.Crater and hill frequency comparison

- Data and Algorithm :

Dynamic Thresholding Algorithm:
We have used a dynamic thresholding algorithm on the DEM data. We have made a histogram of the pixel value distribution and have considered the top 2% of the pixels as a threshold for identifying hills within the terrain data. Similarly, we have considered the bottom 2% of the pixels for identifying craters.

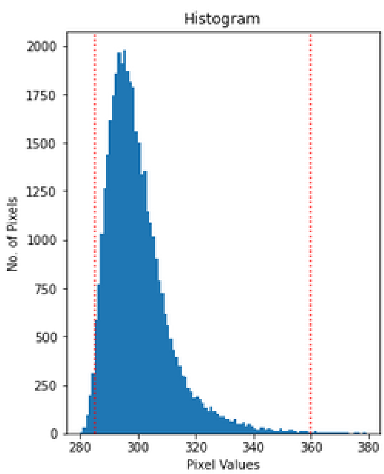

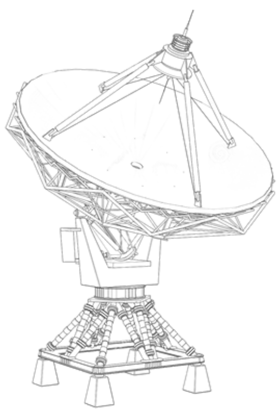

Histogram of pixel values

- Results: We have obtained the results for the craters and depressions detected using dynamic thresholding for both the original images and the super resolved images. [Link to code]

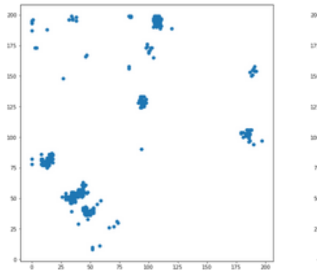

Original Image (Low Altitude Terrain)

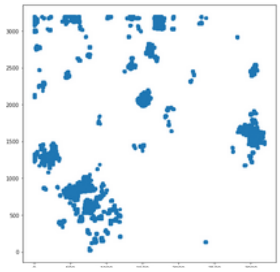

Super Resolved Image (Low Altitude Terrain)

- Inference: We can infer from these results that there is an increase in the frequency of craters being detected in the case of the super-resolved images. This is evident due to the increase in the number of small or misshaped craters which were not well resolved in the original images and hence could not be detected properly. However, the large-scale features remain the same. We can infer from this that the super-resolution is not involuntarily affecting the existing features which were already well-resolved. Thus, there is a tangible increase in the quality of data available for counting craters in case of the super-resolved images.

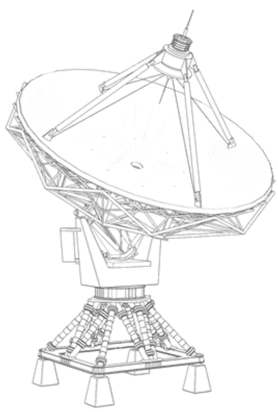

2. Slope and Terrain of craters

- Data and Algorithm: The gradient of the lunar terrain has been studied using the Depth Elevation Map (DEM) data. The heat map of the terrain gradient has been studied for both the original images and the super resolved images. The RichDEM python pipeline has been used for rendering the super resolved images. Furthermore, using the gradient map as a reference a three-dimensional plot of a spatially dynamic region of the DEM data has been generated to gain a deeper understanding of the ways in which the terrain in affected upon super-resolution.

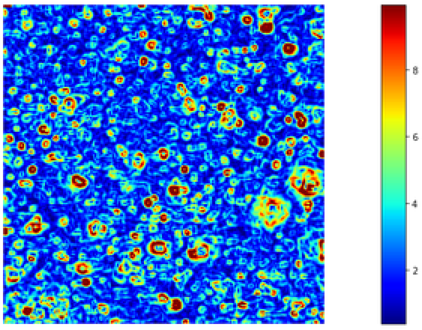

Gradient Map (Original Image)

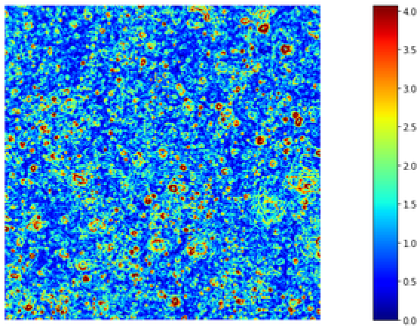

Gradient Map (Super-resolved Image)

- Results: We observe that the super resolution is free from defects and has a finer topology reminiscent of the lunar surface, hence suggesting that our super resolution pipeline can also be employed for DEM maps.

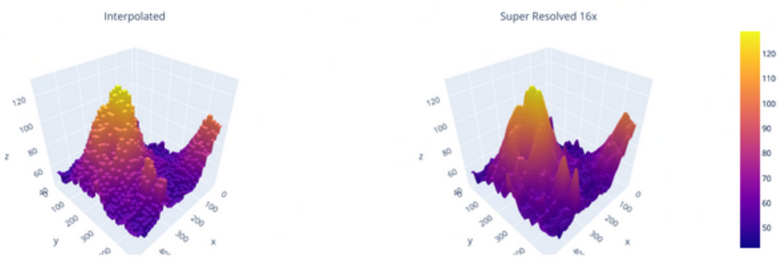

- Inference: The super resolution of the DEM data provides a highly accurate projection of the lunar terrain. This can greatly help in planning future lunar missions and determining locations for rover and manned mission landings.

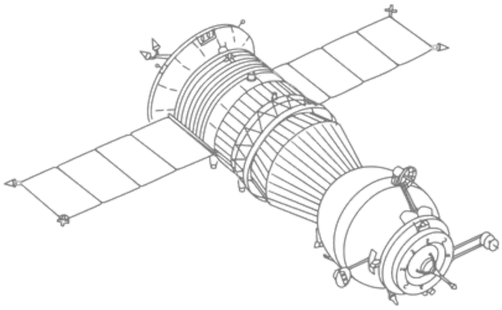

2. Atlas generation

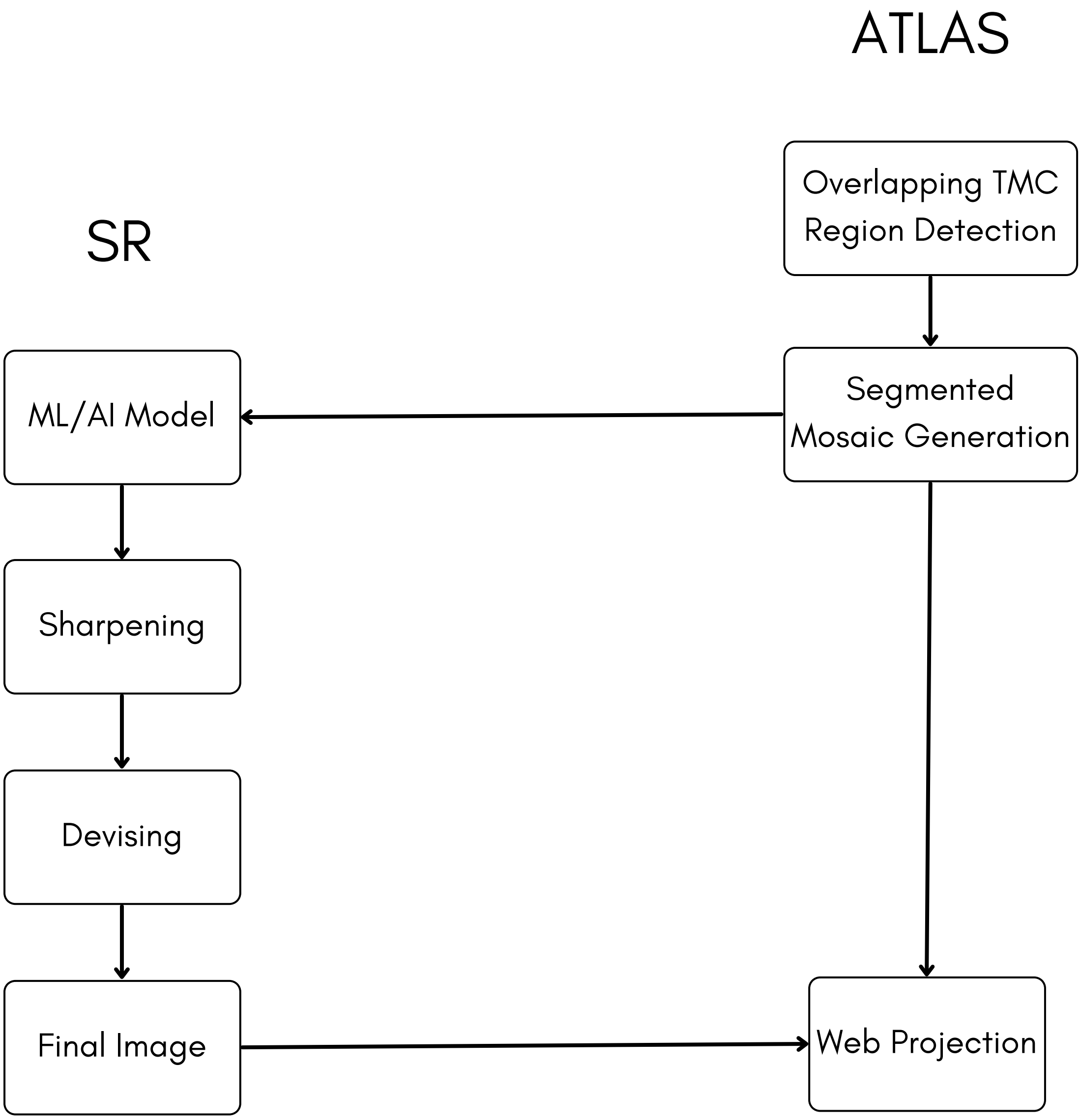

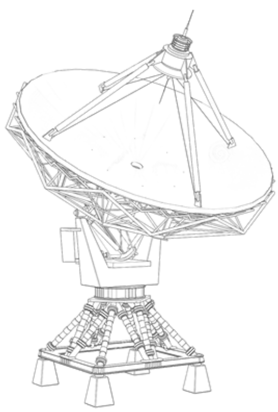

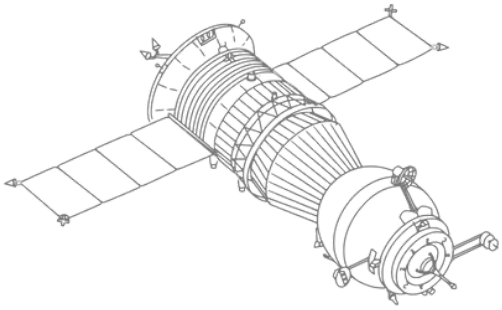

Overlapping TMC region detection

Every TMC file has a corresponding XML file which contains information regarding the coordinates that are mapped in the image. We have used the coordinates labeled as “Corrected coordinates” for this analysis. We have divided the entire lunar atlas, which ranges from -180° to +180° in longitude and -90° to 90° in latitude, into tiles of 20°x20°. Now, we curated a list of all the TMC files that lie in the particular 20°x20° tile for all tiles. We also compute the coordinates of the polygon created by the TMC-tile overlap.

Segmented Mosaic stitching

We then resized all TMC files to have the same number of pixels per degree of the image. Then we created an empty array corresponding to the tile and began populating it with the overlapping parts of the image one by one. Images are pasted one on top of the other while ensuring the null values around the lunar data in the image are replaced by the underlying image. This is done in order to remove the black borders present in the TMC images. Additionally, we calculate the average non zero pixel value for each image in the tile. We take the median value of the images as a reference value and normalize all images to it. This is done to ensure all TMC strips are of equal brightness. Furthermore, we extend the same algorithm to normalize brightness across all 20°x20° tiles.